ACS APPLIED MATERIALS & INTERFACES

Research Article

www.acsami.org

Biobar-Coded Gold Nanoparticles and DNAzyme-Based Dual Signal Amplification Strategy for Ultrasensitive Detection of Protein by Electrochemiluminescence

Hui Xia,[†,‡] Lingling Li,[‡] Zhouyang Yin,[‡] Xiandeng Hou,[†,§] and Jun-Jie Zhu*[,‡]

[†]College of Chemistry and [§]Analytical & Testing Center, Sichuan University, Chengdu, Sichuan 610064, China

[‡]State Key Laboratory of Analytical Chemistry for Life Science, School of Chemistry and Chemical Engineering, Nanjing University, Nanjing 210093, China

Supporting Information

ABSTRACT: A dual signal amplification strategy for electrochemiluminescence (ECL) aptasensor was designed based on biobar-coded gold nanoparticles (Au NPs) and DNAzyme. CdSeTe@ZnS quantum dots (QDs) were chosen as the ECL signal probes. To verify the proposed ultrasensitive ECL aptasensor for biomolecules, we detected thrombin (Tb) as a proof-of-principle analyte. The hairpin DNA designed for the recognition of protein consists of two parts: the sequences of catalytical 8−17 DNAzyme and thrombin aptamer. Only in the presence of thrombin could the hairpin DNA be opened, followed by a recycling cleavage of excess substrates by catalytic core of the DNAzyme to induce the first-step amplification. One part of the fragments was captured to open the capture DNA modified on the Au electrode, which further connected with the prepared biobar-coded Au NPs-CdSeTe@ZnS QDs to get the final dual-amplified ECL signal. The limit of detection for Tb was 0.28 fM with excellent selectivity, and this proposed method possessed good performance in real sample analysis. This design introduces the new concept of dual-signal amplification by a biobar-coded system and DNAzyme recycling into ECL determination, and it is promising to be extended to provide a highly sensitive platform for various target biomolecules.

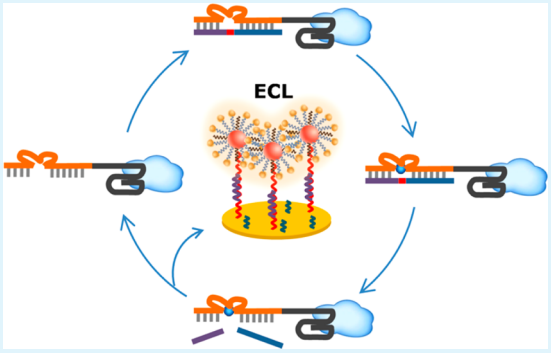

KEYWORDS: *biobar-coded Au NPs, CdSeTe@ZnS QDs, 8−17 DNAzyme, dual signal amplification, electrochemiluminescence, protein*

INTRODUCTION

The trace analysis and quantification of biomolecules such as DNA and protein are closely related to human health as well as the biological activities.[1,2] However, as the concentrations of the biomolecules during the process of disease diagnosis and life exploring are usually very low in living bodies, higher sensitive methods for the detection of these biomolecules are still in demand. Benefiting from the relatively low background and high sensitivity, electrochemiluminescence (ECL) as one of the powerful electrochemical techniques has been widely employed in bioanalysis.[3−5] Since Bard's group reported the stable ECL from Si QDs in 2002,[6] QDs have rapidly become one of the most popular ECL species[7] and biomolecular determinations based on ECL generated by QDs have been widely reported. Taking thrombin as a model protein, previous reports fabricated "sandwich type" biosensors by employing two different types of antithrombin aptamers labeled with efficient signal materials,[8,9] and the ECL quenching systems were established based on the competing reaction between thrombin and complementary DNA with modified QDs and other probes.[10,11] To improve the sensitivity of ECL detection, there are some new methods, such as a multiple DNA cycle amplification strategy[12] and DNA cycle device onto magnetic microbeads (MB).[13] Nanoparticle-based system, the so-called biobar-coded nanoprobe, has been employed as an amplified mode for the development of highly sensitive biosensors. Typically, Au NPs have attracted considerable attention because of their high specific surface area, stability, and biocompatibility. Hundreds of thiolated DNA can be strongly bound at gold surface through Au-thiol binding, whereas signal probes are bound to the other side of DNA strand through different modified functional groups to obtain amplified signals. So far, the biobar-coded Au NP system bound with Ag NPs, $[Ru(NH_3)_6]^{3+}$, quantum dots (QDs), and other signal probes has been applied in various detection technologies, such as mass spectrometry,[14] chemluminescence (CL),[15,16] fluorescence (FL),[17] anodic stripping voltammetry (ASV),[18] electrochemiluminescence (ECL),[19] and so on. Therefore, to further improve the sensitivity, the amplification by biobar-coded Au

Received: October 10, 2014
Accepted: December 5, 2014
Published: December 5, 2014

NPs connecting with QDs is an ideal way to fabricate ECL biosensors.

Recently, DNA enzymes (DNAzymes), isolated from combinatorial oligonucleotide libraries by in vitro selection, have also received great attention because of their better stability than protein enzymes.[20−22] As the activation of DNAzyme could amplify the signal unit by multiple cleavages of substrate strand, several DNAzyme probes were used to develop different amplified strategies for DNA detection.[23−26] Furthermore, combination of aptamer and DNAzyme has also been reported, which opened a new door for the detection of proteins based on DNAzyme amplification via recycling cleavage process.[27,28] Although plenty of methods have been reported to improve the sensitivity of ECL detection,[29,30] the signal amplification for ECL based on DNAzyme with above-mentioned recycling strategy has remained to be developed.

Aiming at developing an ideal sensing platform for protein detection as well as improving the sensitivity of ECL biosensors, we combined both biobar-coded Au NPs and DNAzyme into one ECL system for the first time as a dual amplification strategy, and greater enhancement of ECL signal has been achieved because of the additive effects of each amplification step.

Herein, taking advantages of biobar-coded Au NPs and 8−17 DNAzyme amplification, we designed a new dual-amplified ECL sensing system, where thrombin (Tb) was detected as a proof-of-principle protein, the biobar-coded Au NPs-CdSeTe@ZnS QDs (Au NPs-QDs) act as the ECL signal probes. Because only the catalytic core of the DNAzyme played the important role in first-step amplification, the sequences of aptamer could be replaced by other aptamers for different proteins, thus affording a novel universal amplified sensing platform for protein determination. The amplification effect from both biobar-coded Au NPs-QDs and DNAzyme ensured the sensitivity for detecting proteins at ultralow concentrations.

EXPERIMENTAL SECTION

Materials and Apparatus. DNA oligonucleotides used in this work were synthesized and purified by Sangon Biotechnology Co. Ltd. (Shanghai, China), and the substrate oligonucleotide was synthesized by Takara Biotechnology Co. Ltd. (Dalian, China). The oligonucleotides were diluted in pH 8.0, 1 × TE buffer solution (Sunshine Chemicals Company, Toronto, Canada), the sequences of the DNA are shown in Table S1 in the Supporting Information. Tellurium powder (Te), selenium powder (Se) and *N*-hydroxysuccinimide (NHS) were obtained from Acros Organics (New Jersey, USA). Cadmium chloride was obtained from Jinshanting Chemical reagents factory (Shanghai, China). Trisodium citrate and chloroauric acid ($HAuCl_4$) were obtained from Shanghai Reagent Company (Shanghai, China). Zinc acetate was purchased from Meixing Chemical Co. (Shanghai, China). Disodium hydrogen phosphate, potassium dihydrogen phosphate, sodium hydroxide, magnesium chloride, sodium chloride, potassium chloride, calcium chloride, boric acid, and ethylene diamine tetraacetic acid (EDTA) were obtained from Nanjing Chemical Reagents Factory (Nanjing, China). 3-Mercaptopropionic acid (MPA, 99%) was purchased from Alfa Aesar. Tris(hydroxymethyl)aminomethane (Tris) was obtained from Sinopharm Chemical Reagent Co., Ltd. (Beijing China). Thrombin (Tb) was purchased from Haematologic Technologies Inc. (Esses Junction, VT), bovine serum albumin (BSA, ≥98%), myoglobin, trypsin, lysozyme, 1-ethy-3-(3-(dimethylamino)propyl) carbodiimide hydrochloride (EDC), tris(2-carboxyethyl) phosphine (TCEP), 6-mercapto-1-hexanol (MCH), and tween-20 were purchased from Sigma-Aldrich Chemical Co. (St. Louis, MO, USA). Cytochrome C and glutathione (GSH) were purchased from Aladdin Reagent Database Inc. (Shanghai, China). All the chemicals were of analytical grade and used without further purification. Aqueous solutions were prepared with ultrapure water from an Elix 5 Pure Water System (>18 MΩ cm, Millipore, USA).

The ECL emission was detected with a model MPI-E electrochemiluminescence analyzer (Xi'An Remax Electronic Science & Technology Co. Ltd., Xi'An, China) with a conventional three-electrode system in which a platinum wire, a saturated calomel electrode (SCE) and Au electrodes acted as the auxiliary electrode, reference, and working electrode, respectively. The spectral width of the PMT was 200−800 nm and the voltage of the PMT was set at 800 V during the detection process. The electrochemical impedance spectroscopy (EIS) analysis was carried out on an Autolab PGSTAT12 (Eco chemie, BV, The Netherlands) and controlled by FRA 4.9 software, using the same three-electrode system as in the ECL detection with the frequency range of $0.01-1.0 \times 10^5$ Hz. The gels of gel electrophoresis were scanned using a Molecular Imager Gel DocXR (BIO-RAD, USA). An 8% polyacrylamide gel electrophoresis analysis of the products was carried out in 1 × Tris-borate-EDTA at 100 V constant voltage for about 45 min. Ultraviolet−visible (UV−vis) absorption spectra were obtained using a UV-3600 spectrophotometer (Shimadzu). Fluorescence spectra were obtained on a RF-5301PC spectrophotometer (Shimadzu, Kyoto, Japan). High resolution transmission electron microscopy (HRTEM) images were taken using a JEOL 2010 electron microscope at an accelerating voltage of 200 kV. Samples for HRTEM were prepared by placing the dispersed samples solution on a copper film (400 mesh) and then drying under air.

The buffers involved in this work were as followed: the ECL PBS buffer (0.1 M PBS containing 0.05 M $K_2S_2O_8$ and 0.1 M KCl, pH 7.4), the Tris-HCl binding buffer (20 mM Tris-HCl, 1 mM $MgCl_2$, 1 mM $CaCl_2$, 20 mM NaCl, pH 7.4), PBS buffer for Au NPs and QDs linking (0.05 M PBS containing 1 mM $MgCl_2$, 1 mM $CaCl_2$) and wash buffer (20 mM Tris-HCl containing 0.02% Tween 20, pH 7.4).

Preparation of Au NPs. Au NPs with an average diameter of ∼15 nm were prepared using the procedures reported previously.[31] All glassware were thoroughly cleaned in aqua regia, rinsed with ultrapure water, and dried prior to use. Briefly, 500 mL of 1 mM $HAuCl_4$ was brought to a rolling boil, and then 50 mL of 38.8 mM sodium citrate was added with vigorous stirring. After boiling for 10 min, heating was stopped, and stirring was continued for an additional 15 min, then the solution was cooled to room temperature under stirring.

Preparation of CdSeTe@ZnS QDs. The synthetic pathway for the preparation of CdSeTe@ZnS quantum dots was improved according to our previous reports.[32,33] In a typical synthesis, we first prepared CdSeTe clusters following a previously reported protocol. N_2-saturated $CdCl_2$ solution (5 mM, 50 mL) containing 3-mercaptopropionic acid (MPA, 37 μL) was prepared at room temperature (pH 12.2). Then the premixed solutions of freshly prepared NaHTe and NaHSe with a Te/Se molar ratio of 83/17 were added into the $CdCl_2$ solution rapidly. After stirring for 1 h, the expected CdSeTe clusters were formed and stored in the refrigerator at 4 °C. For the synthesis of CdSeTe/ZnS core−shell QDs, the CdSeTe clusters were precipitated with ethanol and collected via centrifugation at 6,000 rpm, then redissolved in 50 mL of ultrapure water. Zn^{2+} (0.1 M, 200 μL) and GSH (0.1 M, 400 μL) were added into 20 mL of the CdSeTe cluster solution (pH 10.5). The reaction system was refluxed under microwave irradiation (640 W, 2 h).

Preparation of Biobar-Coded Au NPs-QDs. CdSeTe/ZnS QDs (1 mL, 30 μM) were activated in the presence of 200 μL (4.2 mg mL^{-1}) of EDC and 100 μL (2.1 mg mL^{-1}) of NHS for 15 min. The resultant *N*-hydroxysuccinimide-activated QDs were covalently linked to 3′-NH_2 modified signal DNA (1 OD). The reaction was carried out under gentle mixing for 1 h. Then the conjugates were purified by ultrafiltration through a 30 000 MW size filter and centrifugation at 3000 rpm for 15 min and washed twice with water to remove the nonspecifically bound DNA. Then, the TCEP (200 μL, 10 mM) activated conjugates containing 100 μL of 1 M NaCl were transferred to 1 mL of the prepared Au-NPs colloid solution with gentle shaking for 16 h. The mixture was stored for at least 40 h, followed with centrifugation for at least 25 min at 15,000 rpm. The red precipitate

Scheme 1. Schematic Illustration of the Dual Signal Amplification Strategy-Based ECL Aptasensor for Detection of Thrombin

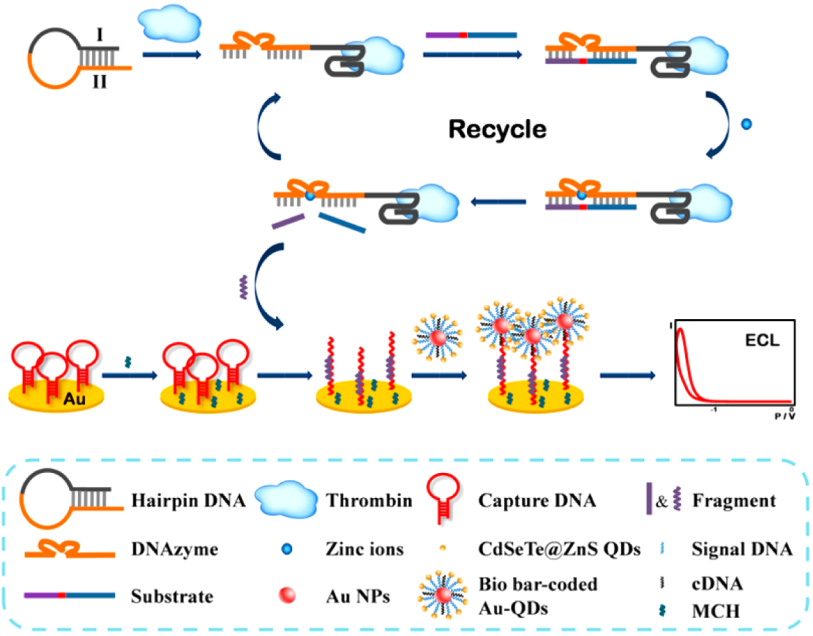

was dispersed in 2 mL of ultrapure water. The TCEP (10 μL, 10 mM) activated complementary DNA (cDNA, 10 μL, 100 μM, signal DNA/cDNA = 90/10) was added into the above-mentioned solution for further reaction under gentle shaking for another 16 h, process of centrifugation and redispersed were repeated. The solution of bio bar-coded Au NPs-QDs was stored at 4 °C.

Procedure for 8−17 DNAzyme Recycle. The hairpin DNA (1 μM) was preactivated at 37 °C for 1 h, then 10 μL of different concentrations of thrombin were added and incubated in Tris-HCl binding buffer at 37 °C for 1 h. Cleavage and recycle reactions were initiated by the addition of the substrate (5 μL, 3 μM) and zinc acetate (1 mM) to the above-mentioned solution to make a final volume of 50 μL with an incubation at 37 °C for 1 h.

Immobilization of Gold Electrode. The polished gold electrode was cleaned with freshly made piranha solution (98% H_2SO_4:30% H_2O_2 = 7:3, v/v) for 20 min, washed with ultrapure water and dried under a nitrogen stream. Ten μL of 3 μM thiolated capture DNA solution was dropped onto the surface of the pretreated gold electrode and kept at 37 °C. Next, the electrode was immersed into 1 mM MCH for 1 h to remove the nonspecifically adsorbed DNA. Then the thiolated capture DNA functionalized electrode was immersed into the prepared solution after recycle at 37 °C for 1 h to capture the signal cleavage. Finally, 10 μL of the prepared cDNA modified bio bar-coded Au NPs-QDs was dropped onto the surface of electrode for further hybridization at 37 °C for 2 h to fabricate the ECL signal probe. During the whole process, the electrode was washed twice with wash buffer after each step of fabrication.

Preparation of Human Serum Samples. The clinical serum samples were from Hospital of Nanjing University. The samples were first diluted for 20 times with binding buffer and then centrifugated by ultrafiltration through a 50 000 Da filter at 6000 rpm for 20 min. Finally, different concentrations of Tb were added into the pretreated human serum. All the experimental conditions and processes were the same as those for the detection of Tb standards.

RESULTS AND DISCUSSION

Principle of the Designed Biobar-Coded Au NPs and DNAzyme Amplification-Based Aptasensor. As shown in Scheme 1, the system mainly consists of a hairpin DNA, a substrate strand, a 3′-thiol-modified capture DNA probe attached to a gold electrode, and the biobar-coded Au NPs-QDs with complementary DNA (cDNA). The hairpin DNA includes two parts, a sequence of 8−17 DNAzyme (orange, part I) and an aptamer sequence (gray, part II) for Tb. To ensure the catalytic activities of the DNAzyme, we designed the sequence of part I according to previous report.[34] After the target Tb was introduced into the system and opened the hairpin DNA by the specific binding between Tb and its aptamer, the substrate strand could hybridize with the opened DNAzyme to make a double-stranded DNA. Compared with Pb^{2+}, which is accepted to be more selective toward 8−17 DNAzyme, Zn^{2+} owns lower toxicity and better solubility, as well as good catalytic effect for the designed DNAzyme at a relatively high concentration,[22] so Zn^{2+} was chosen as a cofactor of the DNAzymes in this work. In the presence of Zn^{2+}, the hydrolytic cleavage took place, and this cleavage resulted in two single-stranded nucleic acids with lower affinity with the DNAzyme, one of which acted as the probe to open the capture DNA on the gold electrode. Then, the DNAzyme could bind to another substrate to make a recycle for the hydrolysis of multiple substrates. The binding process between hairpin DNA, thrombin, and substrate strand was further investigated by gel electrophoresis, the results were shown in Figure S1 in the Supporting Information. The multiple fragments captured on the electrode significantly increased the amount of opened capture DNA and thus realized the first-step signal amplification. Further, the redundant part of opened capture DNA hybridized with the cDNA modified on the biobar-coded Au NPs-QDs, and the CdSeTe@ZnS QDs linked to the Au NPs provide second-step amplification for the final ECL signal.

Characterization of Au-NPs, CdSeTe@ZnS QDs, and Biobar-Coded Au NPs-QDs. The size of Au NPs was estimated from the HRTEM images with an average diameter of about 15 nm (see Figure S2 in the Supporting Information). The representative HRTEM image of the CdSeTe@ZnS QDs has been shown in Figure 1b. The HRTEM image showed the CdSeTe@ZnS QDs are highly crystalline with continuous lattice fringes throughout. The diameters of the QDs are mainly distributed in the range of 2−4.5 nm with an average diameter of 3.3 nm, and the emission wavelength was at 632 nm (see

dx.doi.org/10.1021/am506980d | ACS Appl. Mater. Interfaces 2015, 7, 696−703

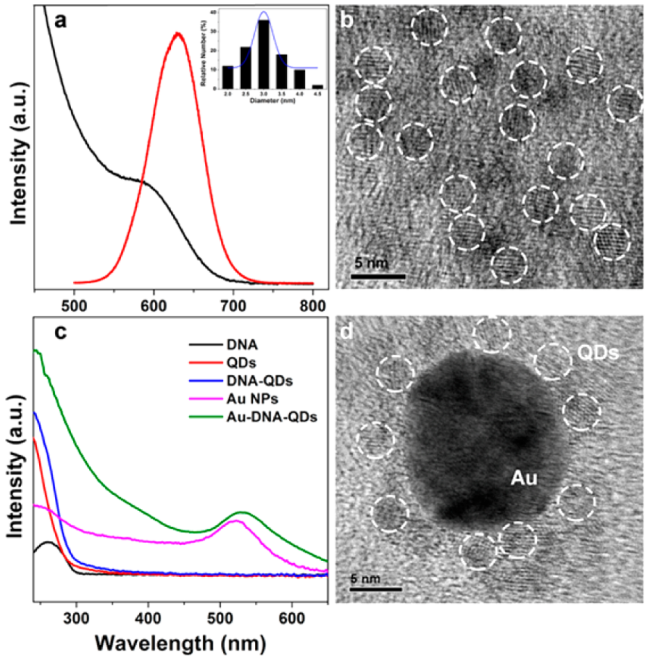

Figure 1. (a) UV–vis absorption spectrum and PL spectrum of the products of CdSeTe@ZnS QDs, size distribution of the CdSeTe@ZnS QDs (inset); (b) HRTEM image of the CdSeTe@ZnS QDs; c, UV–vis extinction spectra of DNA, QDs, DNA-QDs, Au NPs, and Au-DNA-QDs core–satellite; (d) the HRTEM image of a biobar-coded Au NPs-QDs nanoprobe.

Figure 1a). As shown in Figure 1c, the biobar-coded Au NPs-QDs shows combined extinction spectroscopic features of the Au core, the signal DNA linkers, and the QDs, which indicates the successful connecting of Au NPs and QDs by signal DNA. The HRTEM image of CdSeTe@ZnS QDs linked with Au-NPs through 5′-thiol, 3′-amino-modified signal DNA is shown in Figure 1d. The black particles were Au NPs and the light-colored particles exhibiting clear lattice fringes were CdSeTe@ZnS QDs, the image shows that the QDs are assembled around the Au NPs surface.

EIS Characterization. As shown in Figure 2, the whole modification processes were investigated by EIS. Compared with the resistance of bare Au electrode (curve a in Figure 2), the capture DNA and MCH-modified Au electrode showed larger *eT* resistances (curve band c in Figure 2) because of the electrostatic repulsion between negative charges of the DNA and the $[Fe(CN)_6]^{3-/4-}$ redox probe. This *eT* resistance was further enlarged after the modified electrode was immersed into the solution by recycling for the capture of the fragment (curve d in Figure 2). When the biobar-coded Au NPs were successfully bonded to the above electrode, a largest resistance value (curve e in Figure 2) was observed, which may be from the electrostatic repulsion of negative-charged CdSeTe@ZnS QDs.

Feasibility. To verify the feasibility of the proposed dual signal amplification strategy, the ECL behaviors of each amplified steps were investigated (see Table S2 in the Supporting Information). As shown in Figure 3, the direct addition of the mixture of hairpin DNA, substrate and Zn^{2+} onto the capture DNA modified Au electrode could not cause any change in ECL signal (b) in comparison with the capture DNA modified Au electrode background (a), which indicated the hairpin DNA could only be opened by thrombin with the

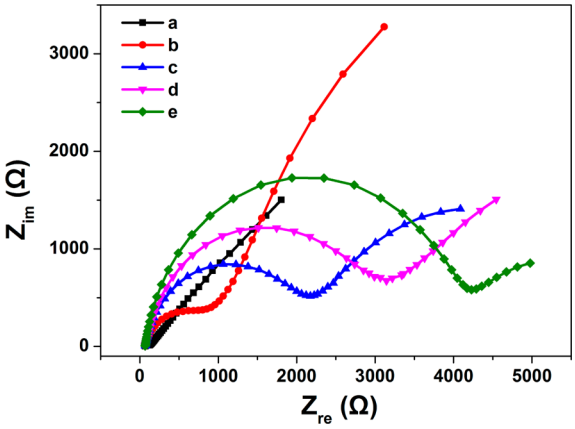

Figure 2. EIS of modified Au electrode at different stages: (a) bare Au electrode; (b) capture DNA/Au electrode; (c) MCH/capture DNA/Au electrode; (d) fragment of substrate/MCH/capture DNA/Au electrode; and (e) biobar-coded Au NPs-QDs/fragment of substrate/MCH/capture DNA/Au electrode. The electrolyte for EIS detection was 0.1 M KCl + 2 mM $[Fe(CN)_6]^{3-}/[Fe(CN)_6]^{4-}$.

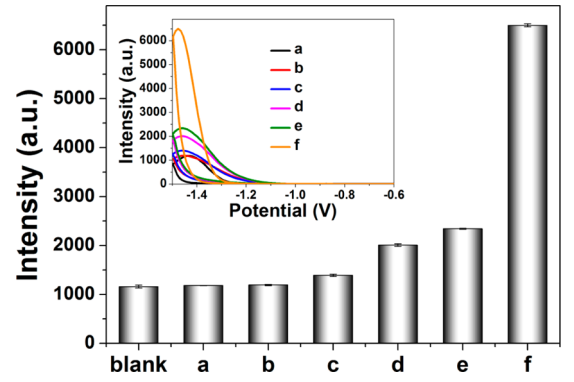

Figure 3. ECL signal of: (a) capture DNA-modified Au electrode; (b) capture DNA-modified Au electrode with the addition of hairpin DNA, substrate, and Zn^{2+}; (c) CdSeTe@ZnS QDs without any amplification; (d) CdSeTe@ZnS QDs with recycling amplification only; (e) biobar-coded Au NPs-QDs without recycling amplification; and (f) biobar-coded Au NPs-QDs with recycling amplification, inset: ECL–potential curves of stepwise amplification.

aptamer sequence. The result was in agreement with the calculated result according to the designed DNA sequences, and it was also proven by electrochemical impedance spectroscopy (EIS, Figure S3 in the Supporting Information) for the difference in resistance of electrode with and without thrombin. In addition, no nonspecific adsorption of thrombin was observed. Several comparisons were introduced to further investigate the amplification effects. First, 1 nM thrombin was added into the same concentration of hairpin DNA and substrate (1 nM, without recycling amplification). After the fragments were captured on the Au electrode, a gentle increase in ECL signal was generated by CdSeTe@ZnS QDs without Au NPs enrichment (c). Notably, the signal was too weak for further application. Second, after the DNAzyme recycle amplification (d), the ECL signal enrichment of CdSeTe@ZnS QDs has only doubled. Third, keeping the concentration of substrate at 1 nM (1:1 with thrombin), the biobar-coded Au NPs modified with CdSeTe@ZnS QDs have been connected to the opened capture DNA, resulting in an enhanced ECL signal (e). Au NPs could enrich the amount of QDs and improve the

dx.doi.org/10.1021/am506980d | ACS Appl. Mater. Interfaces 2015, 7, 696–703

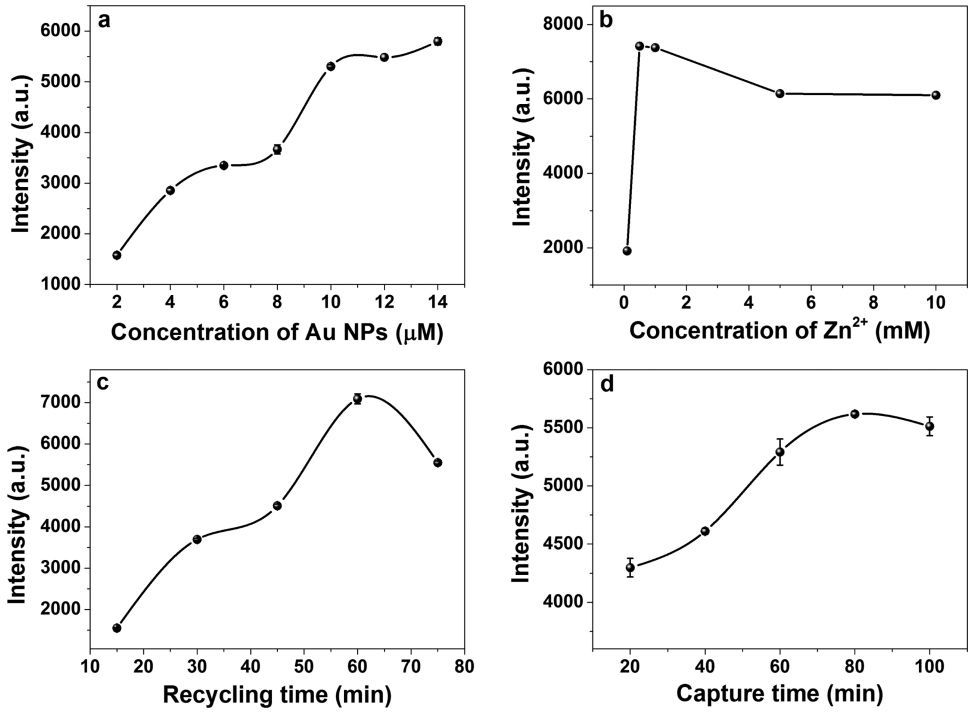

Figure 4. Optimization of experimental conditions: a concentration of biobar coded Au NPs-QDs; (b) concentration of Zn^{2+}; (c) recycling time; and (d) capture time with 3 μM of capture DNA and 1 nM thrombin for determination. When one parameter changes, the others are under their optimal conditions. Error bars were calculated from triple parallel experiments.

conductibility of the electrode surface at the same time, thus amplifying the ECL signal. However, the cleavages captured on the electrode without recycling amplification were at a very low amount, which restricted the connecting amount of biobar-coded Au NPs-QDs. Finally, after combination of both DNAzyme recycling and biobar-coded Au NPs-QDs amplification, the ECL signal was significantly enhanced for about 5 times (f). The result showed that the cooperation of two-step amplification could improve the performance of the ECL system to a large extent by ensuring the amount of both captured fragments and signal QDs. Thus, the proposed dual signal amplification strategy was fantastic for further detection of thrombin.

Optimization of Concentration of Capture DNA, Biobar-Coded Au NPs-QDs and Zn^{2+}. The amount of substrate and degree of the amplification at recycle step were directly determined by the concentration of capture DNA, it was depended on the effective assembling of 3′-thiol-modified capture DNA onto the gold electrode surface by Au−S bond. As shown in Figure S4 in the Supporting Information, the *eT* resistance of the modified electrode increased with the increasing concentration of capture DNA and reached a plateau after 3 μM. As a result, a concentration of capture DNA at 3 μM was the maximum to assemble on the electrode, and the same concentration of substrate strand was chosen for further use.

Under the premise of excess cDNA, the signal responses was obviously effected by the concentration of biobar-coded Au NPs-QDs, which was quantified and calculated by the concentration of Au NPs. The concentration of QDs labeled on Au NPs was about 12 times higher than Au NPs estimated from the concentration of QDs before and after linked with Au NPs. The biobar-coded Au NPs-QDs was concentrated by centrifugation and redissolved with different volumes of PBS buffer. As shown in Figure 4a, the ECL signal reached saturation at the concentration of 10 μM, which was used for further work.

The cleavage rate grows faster with the increase of the concentration of Zn^{2+}. On the other hand, the hybridization efficiency might also be influenced by the Zn^{2+} ion and a high Zn^{2+} concentration was undesirable for the dissociation of the two fragments after DNAzyme cleavage.[26] So the effect of Zn^{2+} concentration was investigated. Figure 4b showed the influence of Zn^{2+} concentration from 0 to 10 mM on the ECL signal. The highest signal response was obtained with the concentration of Zn^{2+} ions at 1 mM and a further increase of the concentration resulted in a slight decrease in signal. Therefore, the optimal concentration of Zn^{2+} ions was 1 mM in buffer.

Optimization of the Recycling Time and the Capturing Time. The recycling time was defined as the incubation time of the mixture of hairpin DNA, thrombin, substrate, and Zn^{2+} ions. Figure 4c showed the dependence of the ECL intensity on recycling time in the presence of 1 nM thrombin. The ECL intensity increased with the increase of the recycling time and then tended to decrease slightly after 60 min, which indicated equilibrium between the cleavage and hybridization. Therefore, a recycling time of 60 min was selected in the following experiments to obtain a high sensitivity. At lower concentration of thrombin, as DNAzyme opened selectively for recycle, the fragments after cleavage should also be less to ensure the quantification of target thrombin.

Besides, the capturing time was also investigated to ensure the fully hybridization of the capture DNA and one-half of the substrate sequence (Figure 4d). The longer capturing time resulted in higher signal response in the range of 20 to 80 min, and the signal kept stable after 80 min. By weighing both the sensitivity and total reaction time during the experiment, a

dx.doi.org/10.1021/am506980d | ACS Appl. Mater. Interfaces 2015, 7, 696−703

capturing time of 1 h was selected for the following experiments.

Analytical Characteristics. Figure 5 exhibits ECL responses toward different concentrations of thrombin and

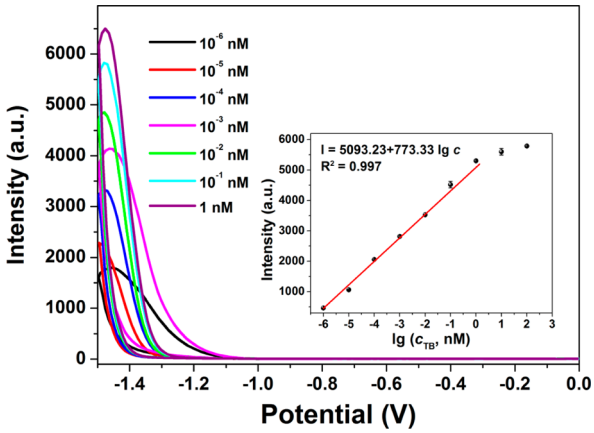

Figure 5. Sensitive detection of Tb: ECL−potential curves of different concentrations of Tb; and inset: calibration curve for Tb determination, with error bars calculated from triple parallel experiments.

the corresponding standard calibration curve for thrombin detection. The ECL response increased accordingly upon increasing the Tb concentration in the range from 0.000001 nM (1 fM) to 1 nM. The regression equation is $I = 773.33\log c + 5093.23$ with a correlation coefficient of 0.997, where I and c represent the ECL intensity and the Tb concentration, respectively. The detection limit was 0.28 fM (S/N = 3). Compared with recently reported aptasensor based on different ECL systems for Tb detection,[35] the designed biosensor with dual signal amplification strategy showed a better sensitivity.

Selectivity and Stability. The ECL aptasensor has good specificity according to the design of hairpin DNA with the sequence of Tb aptamer. To evaluate this property, we chosen five proteins (trypsin, cytochrome c, lysozyme, BSA, and myoglobin) with the concentration of 100 nM to be tested under the same experimental conditions as those for Tb (1 nM). The mixture composed of these interferences (100 nM, respectively) and Tb (1 nM) was also determined for comparison. Obviously, only the presence of Tb (1 nM) led to a significant increase in ECL intensity compared with the presence of the interferences (Figure 6a), suggesting that the proposed aptasensor had good specificity to Tb. Figure 6b shows the ECL intensity of the aptasensor in the presence of 1 nM Tb under continuous scans for 11 cycles. Stable and high ECL signals were observed, which shows that the aptasensor possessed good stability. To evaluate the batch-to-batch variations for preparing the biobar-coded Au NPs, we have compared ECL signals of two batches of biobar-coded Au NPs-QDs used in the work in Figure S5 in the Supporting Information. The results indicated the repeatability of biobar-coded Au NPs-QDs synthesis.

Detection of Thrombin in Human Serum. We further evaluated the applicability of the developed aptasensor by analyzing real samples of complicated matrix. Three concentrations of Tb (0.00001, 0.001, and 0.1 nM) were added into 20-fold diluted human serum. The recovery values were determined under the same experimental conditions as those for Tb and the results were acceptable (Table 1). Therefore, the proposed dual-amplification ECL aptasensor could potentially be applied to real biological samples.

Table 1. Determination of Tb in Real Human Serum Samples

sample	add (nM)	found (nM)	recovery (%)
1	1×10^{-5}	9.95×10^{-6}	99
2	1×10^{-3}	9.71×10^{-4}	97
3	0.1	0.108	108

CONCLUSIONS

By taking biobar-coded Au NPs-QDs and DNAzyme amplification strategies into one ECL system, we demonstrated an ECL aptasensor which was ultrasensitive and selective for detection of thrombin in real samples. The advantages are as follows: (1) this method introduced amplification strategies based on both biobar coded Au NPs for QDs enrichment and DNAzyme recycling into one ECL system for the first time; (2) with the effect of dual amplification, this method achieved

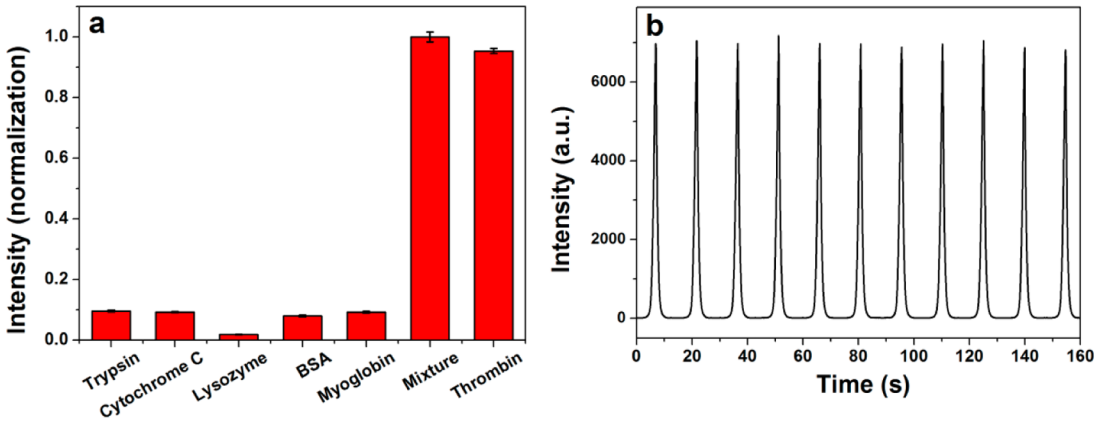

Figure 6. (a) Selectivity investigation for Tb (1 nM) detection against the interference proteins, trypsin (100 nM), cytochrome C (100 nM), lysozyme (100 nM), BSA (100 nM), myoglobin (100 nM), and mixture (containing 1 nM Tb, 100 nM trypsin, 100 nM cytochrome C, 100 nM lysozyme, 100 nM BSA, and 100 nM myoglobin); and (b) the ECL stability of the proposed aptasensor under continuous cyclic voltammetry scan with Tb concentration of 1 nM.

dx.doi.org/10.1021/am506980d | ACS Appl. Mater. Interfaces 2015, 7, 696−703

excellent sensitivity with the LOD of 0.28 fM for thrombin detection; (3) it built the bridge between biomolecules determination and sensitive ECL technology through fragments capture and realized the selective detection of protein by simply connecting of catalytical DNAzyme sequences and selective aptamar sequences; (4) the QDs capped with ZnS used in the aptasensor was harmfulless and the Zn^{2+}, as the cofactor of DNAzyme instead of toxic Pb^{2+}, was more environmentally friendly. Thus, this design principle of amplified analysis followed by ECL determination can be extended to provide a highly sensitive platform for various target biomolecules.

■ ASSOCIATED CONTENT

Supporting Information

DNA oligonucleotides sequence used in this work; Agarose gel electrophoresis analysis; Typical TEM image and UV−vis absorption spectrum of the prepared Au NPs; EIS of substrate modified Au electrode with or without thrombin; EIS of different concentration of capture DNA on Au electrode; ECL signals of batch-to-batch variations for preparing the biobar-coded Au NPs-QDs. This material is available free of charge via the Internet at http://pubs.acs.org/.

■ AUTHOR INFORMATION

Corresponding Author

*Fax & Tel: 0086-25-83594196. E-mail: jjzhu@nju.edu.cn;.

Notes

The authors declare no competing financial interest.

■ ACKNOWLEDGMENTS

This work was supported by National Basic Research Program of China (2011CB933502) and National Natural Science Foundation of China (21335004, 21505078).

■ REFERENCES

(1) Fields, S. Proteomics-Proteomics in Genomeland. *Science* **2001**, *291*, 1221−1224.
(2) Liu, J.; Cao, Z.; Lu, Y. Functional Nucleic Acid Sensors. *Chem. Rev.* **2009**, *109*, 1948−1998.
(3) Miao, W. J. Electrogenerated Chemiluminescence and Its Biorelated Applications. *Chem. Rev.* **2008**, *108*, 2506−2553.
(4) Chen, X. M.; Su, B. Y.; Song, X. H.; Chen, Q. A.; Chen, X.; Wang, X. R. Recent Advances in Electrochemiluminescent Enzyme Biosensors. *Trac-Trends Anal. Chem.* **2011**, *30*, 665−676.
(5) Muzyka, K. Current Trends in The Development of The Electrochemiluminescent Immunosensors. *Biosens. Bioelectron.* **2014**, *54*, 393−407.
(6) Ding, Z. F.; Quinn, B. M.; Haram, S. K.; Pell, L. E.; Korgel, B. A.; Bard, A. J. Electrochemistry and Electrogenerated Chemiluminescence from Silicon Nanocrystal Quantum dots. *Science* **2002**, *296*, 1293−1297.
(7) Wu, P.; H, X. D.; Xu, J.-J.; Chen, H.-Y. Electrochemically Generated versus Photoexcited Luminescence from Semiconductor Nanomaterials: Bridging the Valley between Two Worlds. *Chem. Rev.* **2014**, *114*, 11027−11059.
(8) Huang, H. P.; Zhu, J. J. DNA Aptamer-based QDs Electrochemiluminescence Biosensor for The Detection of Thrombin. *Biosens. Bioelectron.* **2009**, *25*, 927−930.
(9) Xu, W. J.; Wu, Y. M.; Yi, H. Y.; Bai, L. J.; Chai, Y. Q.; Yuan, R. Porous Platinum Nanotubes Modified with Dendrimers as Nanocarriers and Electrocatalysts for Sensitive Electrochemical Aptasensors based on Enzymatic Signal Amplification. *Chem. Commun.* **2014**, *50*, 1451−1453.
(10) Shan, Y.; Xu, J.-J.; Chen, H.-Y. Enhanced Electrochemiluminescence Quenching of CdS:Mn Nanocrystals by CdTe QDs-doped Silica Nanoparticles for Ultrasensitive Detection of Thrombin. *Nanoscale* **2011**, *3*, 2916−2923.
(11) Wang, J.; Shan, Y.; Zhao, W.-W.; Xu, J.-J.; Chen, H.-Y. Gold Nanoparticle Enhanced Electrochemiluminescence of CdS Thin Films for Ultrasensitive Thrombin Detection. *Anal. Chem.* **2011**, *83*, 4004−4011.
(12) Jie, G.; Yuan, J. Novel Magnetic Fe_3O_4@CdSe Composite Quantum Dot-Based Electrochemiluminescence Detection of Thrombin by a Multiple DNA Cycle Amplification Strategy. *Anal. Chem.* **2012**, *84*, 2811−2817.
(13) Guo, Y.; Jia, X.; Zhang, S. DNA Cycle Amplification Device on Magnetic Microbeads for Determination of Thrombin Based on Graphene Oxide Enhancing Signal-on Electrochemiluminescence. *Chem. Commun.* **2011**, *47*, 725−727.
(14) Liu, R.; Liu, X.; Tang, Y. R.; Wu, L.; Hou, X. D.; Lv, Y. Highly Sensitive Immunoassay Based on Immunogold-Silver Amplification and Inductively Coupled Plasma Mass Spectrometric Detection. *Anal. Chem.* **2011**, *83*, 2330−2336.
(15) Zhang, S. S.; Zhong, H.; Ding, C. F. Ultrasensitive Flow Injection Chemiluminescence Detection of DNA Hybridization using Signal DNA Probe Modified with Au and CuS Nanoparticles. *Anal. Chem.* **2008**, *80*, 7206−7212.
(16) Bi, S.; Ji, B.; Zhang, Z.; Zhang, S. A Chemiluminescence Imaging Array for The Detection of Cancer Cells by Dual-aptamer Recognition and Bio-bar-code Nanoprobe-based Rolling Circle Amplification. *Chem. Commun.* **2013**, *49*, 3452−3454.
(17) Zheng, T. T.; Zhang, R.; Zhang, Q. F.; Tan, T. T.; Zhang, K.; Zhu, J. J.; Wang, H. Ultrasensitive Dual-channel Detection of Matrix Metalloproteinase-2 in Human Serum using Gold-quantum Dot Core-satellite Nanoprobes. *Chem. Commun.* **2013**, *49*, 7881−7883.
(18) Hu, K. C.; Liu, P.; Ye, S. J.; Zhang, S. S. Ultrasensitive Electrochemical Detection of DNA based on PbS Nanoparticle Tags and Nanoporous Gold Electrode. *Biosens. Bioelectron.* **2009**, *24*, 3113−3119.
(19) Duan, R.; Zhou, X.; Da, X. Electrochemiluminescence Biobarcode Method Based on Cysteamine-Gold Nanoparticle Conjugates. *Anal. Chem.* **2010**, *82*, 3099−3103.
(20) Li, J.; Lu, Y. A Highly Sensitive and Selective Catalytic DNA Biosensor for Lead Ions. *J. Am. Chem. Soc.* **2000**, *122*, 10466−10467.
(21) Yin, X. B. Functional Nucleic Acids for Electrochemical and Electrochemiluminescent Sensing Applications. *Trac-Trends Anal. Chem.* **2012**, *33*, 81−94.
(22) Zhang, X. B.; Kong, R. M.; Lu, Y. Metal Ion Sensors Based on DNAzymes and Related DNA Molecules. In. *Annu. Rev. Anal. Chem.* **2011**, *4*, 105−128.
(23) Zhao, X. H.; Gong, L.; Zhang, X. B.; Yang, B.; Fu, T.; Hu, R.; Tan, W. H.; Yu, R. Q. Versatile DNAzyme-Based Amplified Biosensing Platforms for Nucleic Acid, Protein, and Enzyme Activity Detection. *Anal. Chem.* **2013**, *85*, 3614−3620.
(24) Sando, S.; Sasaki, T.; Kanatani, K.; Aoyama, Y. Amplified Nucleic Acid Sensing using Programmed Self-cleaving DNAzyme. *J. Am. Chem. Soc.* **2003**, *125*, 15720−15721.
(25) Tian, Y.; Mao, C. D. DNAzyme Amplification of Molecular Beacon Signal. *Talanta* **2005**, *67*, 532−537.
(26) Sun, C. H.; Zhang, L. L.; Jiang, J. H.; Shen, G. L.; Yu, R. Q. Electrochemical DNA Biosensor based on Proximity-dependent DNA Ligation Assays with DNAzyme Amplification of Hairpin Substrate Signal. *Biosens. Bioelectron.* **2010**, *25*, 2483−2489.
(27) Li, D.; Shlyahovsky, B.; Elbaz, J.; Willner, I. Amplified Analysis of Low-molecular-weight Substrates or Proteins by the Self-assembly of DNAzyme-aptamer Conjugates. *J. Am. Chem. Soc.* **2007**, *129*, 5804−5805.
(28) Li, J. S.; Jia, Y. H.; Zheng, J.; Zhong, W. W.; Shen, G. L.; Yang, R. H.; Tan, W. H. Aptamer Degradation Inhibition Combined with DNAzyme Cascade-based Signal Amplification for Colorimetric Detection of Proteins. *Chem. Commun.* **2013**, *49*, 6137−6139.
(29) Hu, L. Z.; Xu, G. B. Applications and Trends in Electrochemiluminescence. *Chem. Soc. Rev.* **2010**, *39*, 3275−3304.

(30) Qi, H. L.; Peng, Y.; Gao, Q.; Zhang, C. X. Applications of Nanomaterials in Electrogenerated Chemiluminescence Biosensors. *Sensors* **2009**, *9*, 674−695.
(31) Grabar, K. C.; Freeman, R. G.; Hommer, M. B.; Natan, M. J. Preparation and Characterization of Au Colloid Monolayers. *Anal. Chem.* **1995**, *67*, 735−743.
(32) Li, L. L.; Chen, Y.; Lu, Q.; Ji, J.; Shen, Y. Y.; Xu, M.; Fei, R.; Yang, G. H.; Zhang, K.; Zhang, J. R.; Zhu, J. J. Electrochemiluminescence Energy Transfer-promoted Ultrasensitive Immunoassay using Near-infrared-emitting CdSeTe/CdS/ZnS Quantum Dots and Gold Nanorods. *Sci. Rep.* **2013**, *3*, 1529.
(33) Shen, Y. Y.; Li, L. L.; Lu, Q.; Ji, J.; Fei, R.; Zhang, J. R.; Abdel-Halim, E. S.; Zhu, J. J. Microwave-assisted Synthesis of Highly Luminescent CdSeTe@ZnS-SiO_2 Quantum Dots and Their Application in The Detection of Cu(II). *Chem. Commun.* **2012**, *48*, 2222−2224.
(34) Zhu, X.; Lin, Z. Y.; Chen, L. F.; Qiu, B.; Chen, G. A. A Sensitive and Specific Electrochemiluminescent Sensor for Lead based on DNAzyme. *Chem. Commun.* **2009**, 6050−6052.
(35) Zhao, M.; Zhuo, Y.; Chai, Y. Q.; Xiang, Y.; Liao, N.; Gui, G. F.; Yuan, R. Dual Signal Amplification Strategy for The Fabrication of An Ultrasensitive Electrochemiluminescenct Aptasensor. *Analyst* **2013**, *138*, 6639−6644.